

## Structure of Monellin Refined to 2.3 Å Resolution in the Orthorhombic Crystal Form

GRZEGORZ BUJACZ,<sup>a</sup> MARIA MILLER,<sup>a</sup> ROBERT HARRISON,<sup>a†</sup> NARMADA THANKI,<sup>a</sup> GARY L. GILLILAND,<sup>b</sup> CRAIG M. OGATA,<sup>c</sup> SUNG-HOU KIM<sup>d</sup> AND ALEXANDER WLODAWER<sup>a\*</sup>

<sup>a</sup>Macromolecular Structure Laboratory, NCI-Frederick Cancer Research and Development Center, ABL-Basic Research Program, Frederick, MD 21702, USA, <sup>b</sup>Center for Advanced Research in Biotechnology of the University of Maryland Biotechnology Institute, and of the National Institute of Standards and Technology, 9600 Gudelsky Drive, Rockville, MD 20850, USA, <sup>c</sup>Howard Hughes Medical Institute, Brookhaven National Laboratory, Upton, NY 11973, USA, and <sup>d</sup>Department of Chemistry and Lawrence Berkeley National Laboratory, University of California, Berkeley, CA 94720, USA. E-mail: wlodawer@ncifcrf.gov

(Received 4 April 1997; accepted 6 May 1997)

### Abstract

The structure of orthorhombic crystals of monellin, a sweet protein extracted from African serendipity berries, has been solved by molecular replacement and refined to 2.3 Å resolution. The final *R* factor was 0.150 for a model with excellent geometry. A monellin molecule consists of two peptides that are non-covalently bound, with chain *A* composed of three β-strands interconnected by loop regions and chain *B* composed of two β-strands interconnected by an α-helix. The N terminus of chain *A* is in close proximity to the C terminus of chain *B*. The two molecules in the asymmetric unit are related by a non-crystallographic twofold axis and form a dimer, similar to those previously observed in other crystal forms of both natural and single-chain monellin. The r.m.s. deviation between the Cα atoms in the two independent molecules is 0.60 Å, while the deviations from the individual molecules in the previously reported monoclinic crystals are 0.50–0.57 Å. This result proves that the structure of monellin is not significantly influenced by crystal packing forces.

### 1. Introduction

Monellin is a small protein that elicits an intensely sweet taste, a property comparatively rare among macromolecules. Isolated from the African plant *Dioscoreophyllum cumminsii* Diels (Morris & Cagan, 1972; van der Wel, 1972), monellin is the principal agent responsible for the sweetness of the plant's berries. This protein is approximately 70 000 times sweeter than sucrose on a molar basis, and is, therefore, together with the protein thaumatin (van der Wel & Loeve, 1972), among the sweetest substances that have been identified so far. The molecular weight of monellin was determined to be 10 700 and the protein was reported to be monomeric in solution, based on the results of gel-filtration chromatography

(van der Wel, 1972; Morris, Martensen, Diebler & Cagan, 1973). A monellin molecule consists of two polypeptide chains; the presence of the N terminus of one chain adjacent to the C terminus of another chain suggested the possibility of engineering a single-chain version of the protein (Kim *et al.*, 1989).

Although orthorhombic crystals of monellin that were obtained more than 20 years ago diffracted well (Wlodawer & Hodgson, 1975), difficulty in preparing heavy-atom derivatives prevented solution of the structure in this crystal form. Subsequently grown monoclinic crystals (Tomlinson & Kim, 1981), however, were used successfully for structure determination. The structure of monellin was originally reported at 3 Å resolution (Ogata, Hatada, Tomlinson, Shin & Kim, 1987) and was later refined to 2.75 Å (Somoza *et al.*, 1993). The limit was imposed by the quality of the crystals, which did not diffract to higher resolution, even with a synchrotron X-ray source. Monoclinic crystals of recombinant single-chain monellin diffracted much better than those of the natural protein and the structure was solved and refined to 1.7 Å resolution. Not surprisingly, the structure of single-chain monellin was shown to be quite similar to that of the natural protein, although some significant differences were reported (Somoza *et al.*, 1993).

Studies of multiple crystal forms of a single protein are useful in defining those structural features that might be influenced by crystal packing, as well as in increasing the overall confidence in the structure. Although in most cases crystal packing does not significantly affect crystal structures (Wlodawer, Nachman, Gilliland, Gallagher & Woodward, 1987), occasionally such influences are significant (Lubkowski *et al.*, 1997). For such reasons, the availability of protein structures obtained in multiple crystal forms can be very useful, especially if some of the structures have been solved at modest resolution, as was the case with natural monellin. We have now solved the structure of natural monellin in the original orthorhombic crystal form, refined it to 2.3 Å resolution and compared it with both of the structures published previously.

† Present address: Jefferson Cancer Institute, Thomas Jefferson University, Philadelphia, PA 19107, USA.

## 2. Materials and methods

### 2.1. Crystal growth

Monellin used in this study was a gift from Dr R. H. Cagan, Monell Institute, Philadelphia. It was isolated from berries of the serendipity plant, purified as described previously (Morris & Cagan, 1972) and delivered as white lyophilized powder. No further purification before crystallization was necessary. Large crystals (over 0.5 mm in each dimension) were obtained by vapor diffusion of 20%(v/v) ethanol into a solution containing 5–10 mg of the protein in 100 mM of sodium phosphate buffer, pH 7.2, using the hanging-drop technique, as described previously (Wlodawer & Hodgson, 1975). Since the crystals were not stable and tended to deteriorate rapidly, before data collection they were crosslinked for 1–1.5 h with 0.015% glutaraldehyde. Crosslinking appeared to stabilize the crystals without loss of diffraction at high resolution, but glutaraldehyde molecules were not seen in the final structure. Interestingly, attempts to grow orthorhombic crystals from a commercial preparation (obtained from Sigma, Lot 121F-3776) were not successful, even after partial purification of the protein on a carboxymethyl cellulose column, although it was possible to grow the monoclinic crystals (Tomlinson & Kim, 1981) from this preparation.

### 2.2. X-ray data collection

X-ray diffraction data were collected at Genex Corporation, Gaithersburg, Maryland, using a Siemens Imaging Proportional Counter (IPC), an electronic area detector mounted on a Supper oscillation camera controlled by a Cadmus 9000 microcomputer. During data collection, the area-detector chamber was mounted at a distance of 10 cm from the crystal. The carriage angle was set at 20°, enabling the detector to intercept data from ∞ to 2.3 Å. Diffraction data collected by the IPC detector were recorded as a series of discrete frames, each comprising a 0.25° oscillation angle counted for 120–160 s. Two orientations of 400 data frames, each corresponding to 100° of crystal rotation, were measured. The X-ray source used to generate Cu K $\alpha$  radiation was an Elliot GX-21 rotating anode, operated at 70 mA and 40 kV with a 0.3 × 3.0 mm focal spot and a 0.3 mm collimator. Monochromatization was provided by a Huber graphite monochromator. All data collection was performed at well controlled room temperature (289–291 K).

### 2.3. X-ray data processing

The determination of crystal orientation and the integration of reflection intensities was performed with the XENGEN program system (Howard *et al.*, 1987). The X-ray diffraction data measured from only one crystal included 36 281 observations of 10 602 unique reflections out of the 11 667 possible at 2.3 Å. The data were scaled with an unweighted least-squares *R* factor on

intensity for symmetry-related observations of 0.066 (Table 1); 7964 of the measured unique reflections had significant intensity [ $F > 2\sigma(F)$ ]. There was no evidence of any significant anisotropy in the diffraction pattern, but the fall-off of the intensity was rapid beyond 3 Å.

### 2.4. Structure solution

The structure of orthorhombic monellin was solved by using molecular replacement methods. The starting model was provided by the structure of monoclinic monellin in a crystal form with four molecules in the asymmetric unit (Ogata *et al.*, 1987). This model was similar, but not identical to the structure deposited at the Brookhaven Protein Data Bank (Bernstein *et al.*, 1977) with accession code 3MON. For the initial calculation of the rotation function, we arbitrarily selected only molecule I from the model. Since two peaks related by an approximately 180° rotation could be seen after rotation-function calculations based on this model, we predicted that the tight dimer seen in the monoclinic crystal form would also be present in the orthorhombic crystals, and thus further work involved coordinates of a dimer made of molecules I and II.

The orientation of the dimer within the unit-cell was found by performing two radically different rotation functions independently: (1) Crowther's fast-rotation function (Crowther, 1972), as implemented in the molecular replacement program package MERLOT (Fitzgerald, 1988), and (2) the real-space version of the Patterson search technique (Huber, 1965), as implemented in the program package PROTEIN (Steigemann, 1974). The fast-rotation-function searches were performed using data from 10 to 3 Å and in steps of 2.5° in  $\alpha$ , and 5.0° in  $\beta$  and  $\gamma$ , where  $\alpha$ ,  $\beta$  and  $\gamma$  are Euler angles as defined by Crowther (1972). A maximum correlation of 4.4 r.m.s. units was found at  $\alpha = 35.1$ ,  $\beta = 92.92$ ,  $\gamma = 159.27^\circ$  and the symmetry-related position  $\alpha = 215.1$ ,  $\beta = 87.08$ ,  $\gamma = 20.73^\circ$ . The next highest peak was 60% of this first one. Changing the grid size did not shift the peak position. A slow-rotation function was run and the highest peak was found to be considerably shifted (at  $\alpha = 20$ ,  $\beta = 93$ ,  $\gamma = 145^\circ$ ) compared with that from the fast-rotation function.

The real-space rotation search, performed in steps of 5.0° in all three Euler angles using data between 15.0 and 3.0 Å resolution, produced a map with a peak of 4.4 r.m.s. units above average at  $\alpha = 20.3$ ,  $\beta = 92.3$ ,  $\gamma = 145.3^\circ$ . The intensity of the next highest peak was 3.2 r.m.s. units, *i.e.* about 72% of the maximum peak height. This peak agrees very well with the one obtained by the application of the slow-rotation function.

The position in the unit-cell of the model resulting from the rotation search was found by using a 'brute force' translation program, TF (J. Remington, unpublished work). The translation search was performed on a grid of 1.0 Å in each direction, using data between 10.0 and 4.0 Å resolution. The resulting map had a maximum

Table 1. *Data collection and refinement statistics for orthorhombic monellin*

Unit-cell parameters	
<i>a</i> (Å)	54.00
<i>b</i> (Å)	112.42
<i>c</i> (Å)	40.05
Space group	<i>P</i> 2 <sub>1</sub> 2 <sub>1</sub> 2
<i>R</i> <sub>merge</sub>	0.066
No. of reflections	
Total (no cut off)	36281
Unique	10602
Used for refinement	7607
[2σ( <i>F</i> ) cut off, 8–2.3 Å]	
Completeness of the data (%)	90.9
No. of protein atoms	1568
No. of solvent atoms	180
Resolution range (Å)	8.0–2.3
<i>R</i> factor	0.150
Mean <i>B</i> factor (Å <sup>2</sup> )	44.25
R.m.s. deviations from ideality	
Bonds (Å)	0.013
Angle distances (Å)	0.033
Plane restraints (Å)	0.011
Chiral volumes (Å <sup>3</sup> )	0.096

of 8.6 r.m.s. units, with a correlation coefficient of 0.436, located at  $x = 0.167$ ,  $y = 0.391$ ,  $z = 0.404$  (in fractions of unit-cell dimensions); the next highest peak was 6.7 r.m.s. units. The set of coordinates corresponding to this solution was used in the refinement.

The initial refinement of the structure was performed with the program *X-PLOR* (Brünger, 1992), first using a rigid-body approximation, then by a slow-cool protocol with a starting temperature of 3000 K. Further refinement was carried out using the program *PROFFT* (Hendrickson, 1985; Finzel, 1987) running in a VMS shell for automatic handling and submission of multiple cycles (M. Jaskólski, unpublished work). The weights used in the refinement were only a function of the resolution of the data; individual standard deviations were not used. Model building between refinement cycles was performed using the graphics program *FRODO* (Jones, 1985) on an Evans & Sutherland PS390 graphics system. The solvent molecules were placed by automatic interpretation of difference Fourier peaks based on stereochemical criteria (M. Jaskólski, unpublished work).

Convergence was reached when the conventional *R* factor became 0.150, for data between 8.0 and 2.3 Å, with excellent stereochemical parameters (the r.m.s. deviation of bond lengths from ideal values was 0.013 Å). Other refinement results are summarized in Table 1. The coordinates and structure factors have been deposited with the Brookhaven Protein Data Bank.†

### 3. Results and discussion

#### 3.1. Refined model

The final refined model of monellin (Fig. 1) contains 94 residues in each of the two molecules in the asymmetric unit, as well as 180 water molecules. The N-terminal phenylalanine, apparently present in only 10% of natural monellin, is not included in the model, since it was not visible in the electron-density map. The model has acceptable geometry, with 97% of residues located in the most preferable regions in the Ramachandran plot (Fig. 2). Three residues in each molecule are located in left-handed  $\beta$ -turns: Ser16 and Asp17 create a sharp turn between the first and second  $\beta$ -strands, and Arg31 is located in the turn between the second and third  $\beta$ -strands, all in chain *A*. The rest of the residues are located in the allowed regions, clustering near ideal  $\beta$ -strand and  $\alpha$ -helix conformations. Strong non-crystallographic symmetry restraints were imposed during the initial refinement, but this protocol was not successful in the later stages of refinement. Clear differences between the molecules required independent model rebuilding, mostly with respect to the conformation of the main chain of the loop containing residues 70–76, of side chains in other areas, and of the interface between the N terminus of chain *A* and the C terminus of chain *B* in the same molecule. In the final structure, the r.m.s. deviation between the C $\alpha$  atoms of the two molecules is 0.60 Å. The protein shows a high degree of flexibility, indicated by a high average *B* factor of 44.25 Å<sup>2</sup>. This high value is

† Atomic coordinates and structure factors have been deposited with the Protein Data Bank, Brookhaven National Laboratory (Reference: 4MON and R4MONSF). Free copies may be obtained through The Managing Editor, International Union of Crystallography, 5 Abbey Square, Chester CH1 2HU, England (Reference: GR0374).

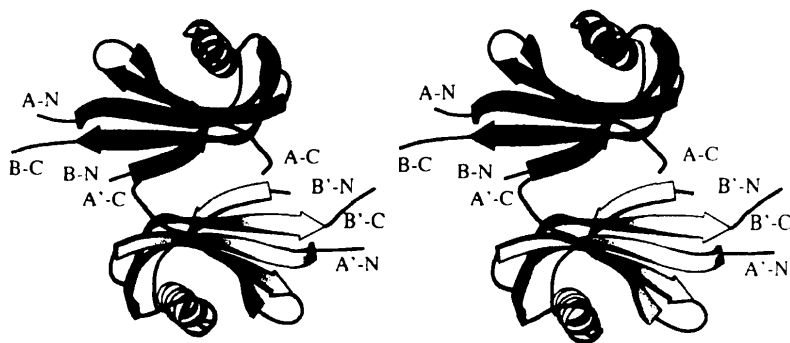


Fig. 1. Stereo diagram of the dimer of orthorhombic monellin, created using *MOLSCRIPT* (Kraulis, 1991). The two molecules are shown in different shades of grey.

undoubtedly related to the general weakness of the diffraction data, as manifested by a comparatively large number of 'unobserved' reflections with intensities less than  $2\sigma(F)$  (Table 1). Not surprisingly, the  $B$  factors are highest at the termini and in the loop regions, and lowest for the regular elements of secondary structure (Fig. 3). The  $B$  factors are also similar for both protein chains, despite their different crystal contacts.

The structure of monellin in orthorhombic crystals is similar to the structure of monoclinic monellin reported previously (Ogata *et al.*, 1987; Somoza *et al.*, 1993). Each molecule of monellin consists of two peptide chains: chain *A* has 45 residues, of which 44 were seen in the electron-density maps, while chain *B* has 50 residues. Chain *A* contains three antiparallel  $\beta$ -strands. Chain *B* is composed of two antiparallel  $\beta$ -strands and one  $\alpha$ -helix. Although chains *A* and *B* are not bound covalently, they interact very closely and together form a five-stranded antiparallel  $\beta$ -sheet draped with a slight twist around the  $\alpha$ -helix. The contacts between the  $\beta$ -sheet and the  $\alpha$ -helix are mainly hydrophobic. The network of hydrogen bonds within the  $\beta$ -sheet (Fig. 4) shows two peculiar irregularities. The first is located in the area of Pro85, which has a *cis* conformation. This *cis* peptide bond forms a bend in the second  $\beta$ -strand in chain *B*, so that two hydrogen bonds that would otherwise have been formed are missing. This conformation of the proline ring allows a close hydrophobic interaction with the aromatic ring in Trp48' from the other molecule. Such interaction plays an important role in the central hydrophobic part of the dimer interface. The second irregularity is observed on the third  $\beta$ -strand of chain *A*, where the carbonyl O atom of Leu36 points into the solvent. Only the N atom of this residue participates in the hydrogen-bond network. The

missing carbonyl hydrogen bond is compensated by a hydrogen bond (2.37 Å long) between the side chains of Arg37 and Asp22 and by an additional hydrophobic interaction between the side chains of Leu35 and Phe38. The central part of the dimer interface contains mostly hydrophobic residues, surrounded by some hydrophilic contacts at the periphery. The hydrophobic interactions are between Ile50 and Ile50' from the other molecule, Met87 and its analog Met87', Trp48 and Pro85', and in the opposite pairing of Trp48' with Pro85. Hydrophilic interactions at the periphery of the dimer interface involve the terminal residues. Carbonyl O atoms from Gly46 create a short hydrogen bond with the NH1 of Arg84' (2.41 Å). An analogous interaction on the opposite side of the non-crystallographic twofold axis is weaker, with a distance of 3.92 Å between O Gly46' and NH1 Arg84. The terminal carboxyl group of chain *A* interacts with the side chain of Lys89' with a distance of 3.52 Å. The distance between the analogous OXT Pro45' and NZ Lys89' is nearly the same at 3.60 Å. Four out of the five C-terminal residues of chain *A* are prolines. In the sequence Pro-Val-Pro-Pro-Pro, the first proline, Pro41, has a *cis* conformation.

The N terminus of chain *A* is close to the C terminus of chain *B* within the same molecule. This property was previously utilized to create the single-chain construct of monellin. These termini show a high degree of flexibility, indicated by their high  $B$  factors and different conformations in each molecule. The C terminus of chain *A* of one molecule and the N terminus of chain *B* of the other molecule in the dimer are also located close together. As noted previously, these termini are linked to the dimer interface by hydrogen bonds and show lower flexibility than the first pair of termini. Another flexible region is the loop connecting the helix with the second  $\beta$ -strand in the *B* chain. This loop is stabilized by interdimer crystal contacts in a different manner and exhibits different conformations in each molecule. Such stabilization is better for the second molecule, as indicated by slightly lower  $B$  factors.

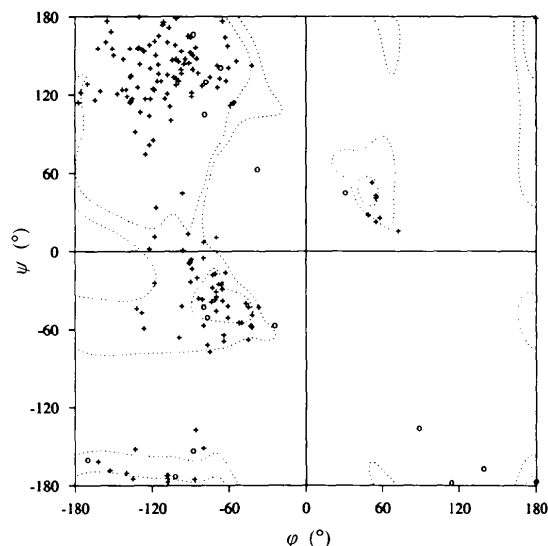


Fig. 2. Ramachandran plot for orthorhombic monellin. All residues are marked by crosses, except glycine and proline, which are marked by circles.

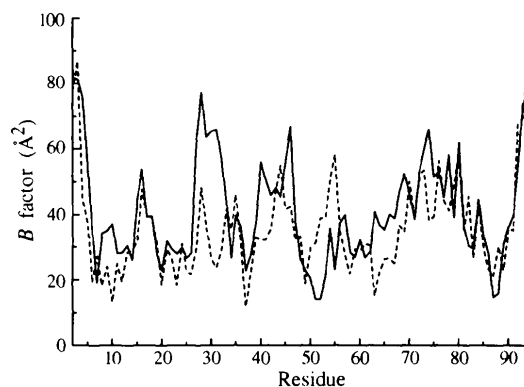


Fig. 3. A plot of r.m.s. displacement parameters for the main-chain atoms in both molecules of orthorhombic monellin. Molecule I is shown by the solid line; molecule II, by the dashed line.

### 3.2. Comparison with other crystal forms

The crystal packing (Fig. 5) found in both crystal forms of natural monellin is not very tight. The  $V_m$  value is  $2.79 \text{ \AA}^3 \text{ Da}^{-1}$  for monoclinic monellin and  $2.84 \text{ \AA}^3 \text{ Da}^{-1}$  for the orthorhombic form. The crystal packing for the engineered single-strand monellin is much more compact, with a  $V_m$  value of  $2.11 \text{ \AA}^3 \text{ Da}^{-1}$ . A very important role in the crystal packing of natural monellin is played by the interactions of the two termini that are not involved in creating the dimer interface contacts. The N terminus of chain *A* and the C terminus of chain *B* point away from the molecule and have high displacement parameters. Additionally, these termini both have long charged side chains, including arginine and glutamic acid, which present the possibility of creating hydrogen bonds. Monellin contains a large number of hydrophilic residues on the surface, which may be why we observe the different crystal forms. The C-terminus residues interact not only with different residues in different crystal forms, but also with different residues of each molecule within each crystal form. Single-stranded monellin has covalently linked termini and only the flexible side chains of arginine and glutamic acid in the engineered region can interact with neighboring molecules. The average displacement parameters are very similar for both crystal forms of natural monellin, while they are significantly lower for the single-chain monellin.

Comparison of each of the two molecules in the orthorhombic monellin with individual molecules found in the monoclinic crystals showed that the r.m.s. deviations between the respective sets of  $C\alpha$  coordinates range between 0.50 and 0.57 Å. The deviations from the coordinates of single-chain monellin range between 0.45 and 0.54 Å. By comparison, the pairwise deviations of the individual chains in monoclinic monellin are approximately 0.3 Å, while the two chains of single-chain monellin differ by 0.52 Å. It is clear that the smallest deviations observed for monoclinic monellin were caused by strong non-crystallographic symmetry restraints, which had to be applied because of the limited resolution of the diffraction data. These comparisons also show that crystal contacts are not the primary source of

differences between the conformations of individual molecules.

Although monellin was reported to be monomeric in solution (van der Wel, 1972; Morris *et al.*, 1973), the dimers observed in different crystal forms are quite similar. The r.m.s. deviation between the dimer in the orthorhombic crystals and dimer 1–2 in the monoclinic crystals is 0.8 Å, although the deviation is 1.24 Å for dimer 3–4. The deviation between the dimer of orthorhombic monellin and single-chain monellin is 0.9 Å. These comparisons show very clearly that the quaternary structure of monellin appears to be preserved between different crystal forms almost as well as its tertiary structure and is not significantly influenced by crystallization conditions, or even by engineering a covalent link between the two chains. Subsequent measurements by dynamic light scattering at 2 and 5 mg ml<sup>-1</sup> concentration have yielded the apparent molecular weight of ~26 000, strongly suggesting the presence of dimers under these conditions (data not shown). While this result explains very well the conservation of the dimer observed in all structures, we do not know the reason for the discrepancy with a previous report of a monomer seen in the native gels (Morris *et al.*, 1973).

### 3.3. Comparison with related proteins

One of the most intriguing questions concerning monellin and other sweet proteins is the identity of the portion of the molecule responsible for the sweet taste. However, the structure of the protein, even in multiple crystal forms, does not reveal directly the regions responsible for binding to the receptors. No definitive clues have been found from the studies of an unrelated sweet protein, thaumatin (Cagan, 1973). Primary structures of these proteins show no detectable homology (de Vos *et al.*, 1985; Ogata *et al.*, 1987; Kim *et al.*, 1989) and their tertiary structures are very different, although both proteins bind to the same receptor and thus should possess structurally similar receptor-binding regions. No three-dimensional structures are available for other, more recently identified sweet proteins, such as pentadin (van der Wel, Hladik, Hladik, Hellikant & Glaser, 1989),

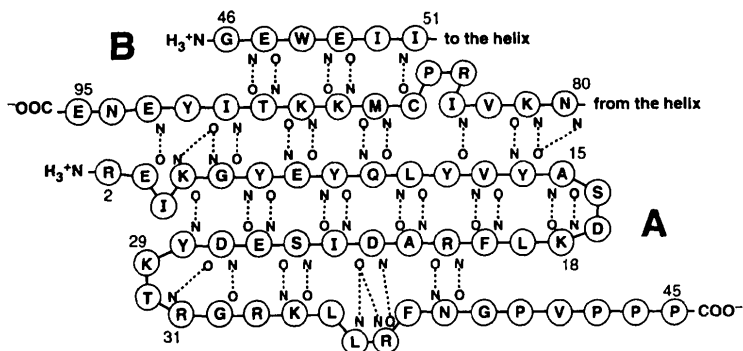


Fig. 4. A diagram showing the hydrogen bonds in the five-stranded  $\beta$ -sheet region for orthorhombic monellin. The diagram shows molecule I; in molecule II the direct hydrogen bond from E3 to E93 is replaced by an indirect hydrogen bond through a water molecule

curculin (Yamashita *et al.*, 1990) or mabinlin (Liu *et al.*, 1993). On the other hand, the cysteine protease inhibitor stefin B and chicken egg-white cystatin have an unexpectedly high similarity of their secondary and tertiary structures to that of monellin, despite having no

functional relationship (Bode *et al.*, 1988; Stubbs *et al.*, 1990; Murzin, 1993; Somoza *et al.*, 1993). Not surprisingly, the chiral structure of monellin is necessary for retaining its sweet taste, since an analog consisting entirely of D amino acids is tasteless (Ariyoshi &

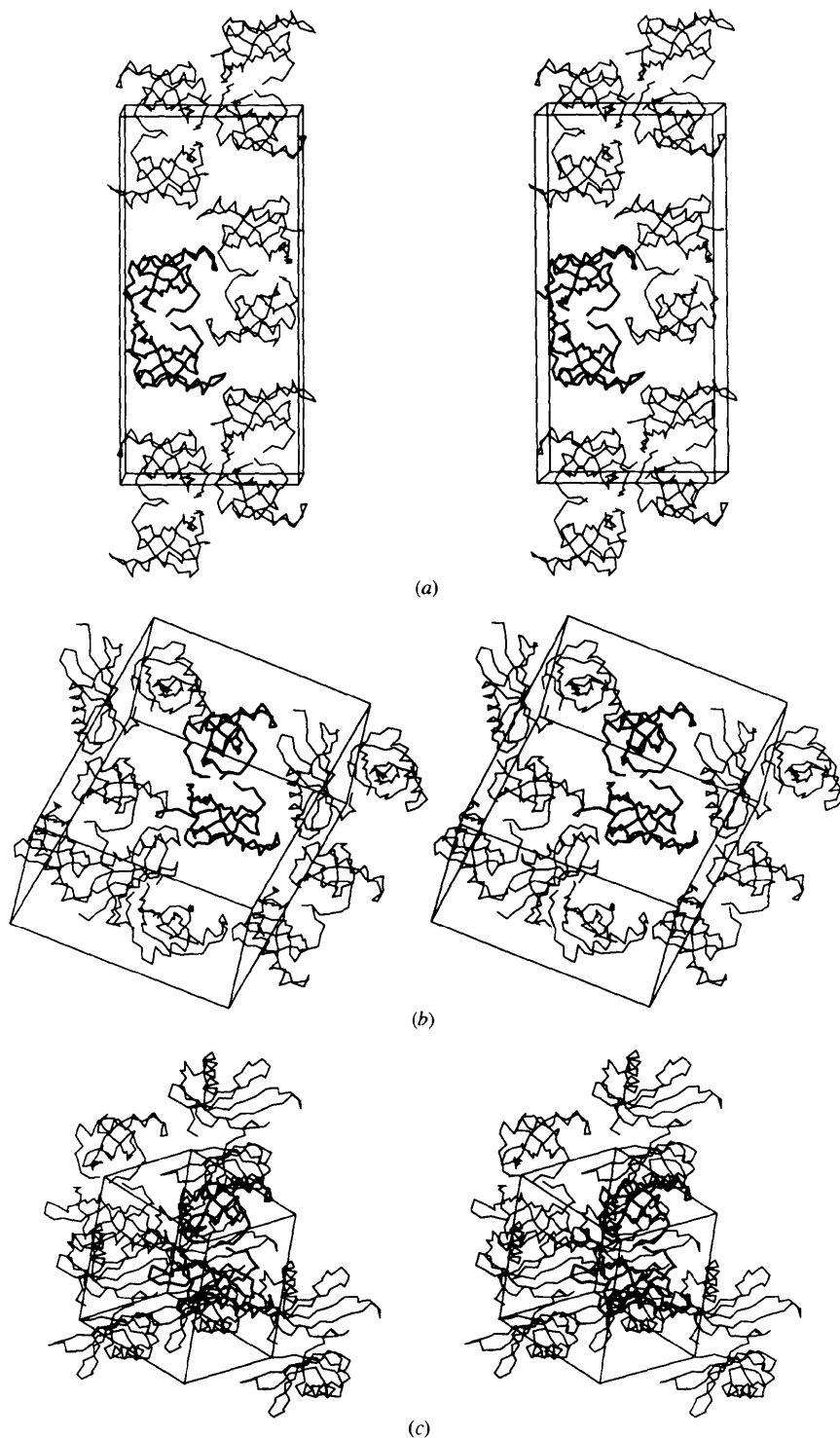


Fig 5. Crystal packing for three different crystal forms of monellin. One of the dimers (shown in bold) is oriented in approximately the same way in all the panels: (a) C $\alpha$  tracing for orthorhombic monellin, viewed approximately along the crystallographic z axis; (b) monoclinic natural monellin; (c) monoclinic single-chain monellin.

Kohmura, 1994). Thus, further experiments are needed to elucidate the structural features responsible for the biological activity of monellin.

We thank Dr R. H. Cagan of the Monell Institute for a gift of purified protein, Dr A. Howard for assistance with data collection and processing, Dr A. Treharne for her contribution to the refinement of the structure, J. Alexandratos for light-scattering measurements, and A. Arthur for editorial comments. This research was sponsored in part by the National Cancer Institute, DHHS, under contract with ABL. The contents of this publication do not necessarily reflect the views or policies of the Department of Health and Human Services, nor does mention of trade names, commercial products, or organizations imply endorsement by the US Government. Certain commercial equipment, instruments, and materials are identified in this paper in order to specify the experimental procedure as completely as possible. In no case does such identification imply a recommendation or endorsement by the National Institute of Standards and Technology nor does it imply that the material, instrument, or equipment identified is the best available for the purpose.

#### References

- Ariyoshi, Y. & Kohmura, M. (1994). *J. Synth. Org. Chem. Jpn.*, **52**, 359–369.
- Bernstein, F. C., Koetzle, T. F., Williams, G. J. B., Meyer, E. F. Jr, Brice, M. D., Rogers, J. R., Kennard, O., Shimanouchi, T. & Tasumi, M. (1977). *J. Mol. Biol.* **112**, 535–547.
- Bode, W., Engh, R., Musil, D., Thiele, U., Huber, R., Karshikov, A., Brzin, J., Kos, J. & Turk, V. (1988). *EMBO J.* **7**, 2593–2599.
- Brünger, A. (1992). *X-PLOR Version 3.1. A System for X-ray Crystallography and NMR*. Yale University Press, New Haven, Connecticut, USA.
- Cagan, R. H. (1973). *Science*, **181**, 32–35.
- Crowther, R. A. (1972). *The Molecular Replacement Method*, edited by M. G. Rossmann, pp. 173–178. New York: Gordon & Breach.
- Finzel, B. C. (1987). *J. Appl. Cryst.* **20**, 53–55.
- Fitzgerald, P. M. D. (1988). *J. Appl. Cryst.* **21**, 273–278.
- Hendrickson, W. A. (1985). *Methods Enzymol.* **115**, 252–270.
- Howard, A. J., Gilliland, G. L., Finzel, B. C., Poulos, T. L., Ohlendorf, D. H. & Salemme, F. R. (1987). *J. Appl. Cryst.* **20**, 383–387.
- Huber, R. (1965). *Acta Cryst.* **19**, 353–356.
- Jones, T. A. (1985). *Methods Enzymol.* **115**, 157–171.
- Kim, S. H., Kang, C. H., Kim, R., Cho, J. M., Lee, Y. B. & Lee, T. K. (1989). *Protein Eng.* **2**, 571–575.
- Kraulis, P. J. (1991). *J. Appl. Cryst.* **24**, 946–950.
- Liu, X., Maeda, S., Hu, Z., Aiuchi, T., Nakaya, K. & Kurihara, Y. (1993). *Eur. J. Biochem.* **211**, 281–287.
- Lubkowsky, J., Bujacz, G., Boque, L., Domaille, P. J., Handel, T. M. & Wlodawer, A. (1997). *Nature Struct. Biol.* **4**, 64–69.
- Morris, J. A. & Cagan, R. H. (1972). *Biochim. Biophys. Acta*, **261**, 114–122.
- Morris, J. A., Martensen, R., Diebler, G. & Cagan, R. H. (1973). *J. Biol. Chem.* **248**, 534–539.
- Murzin, A. G. (1993). *J. Mol. Biol.* **230**, 689–694.
- Ogata, C., Hatada, M., Tomlinson, G., Shin, W. C. & Kim, S. H. (1987). *Nature (London)*, **328**, 739–742.
- Somoza, J. R., Jaing, F., Tong, L., Kang, C.-H., Cho, J.-M. & Kim, S.-H. (1993). *J. Mol. Biol.* **234**, 390–404.
- Steigemann, W. (1974). PhD thesis, Technische Universität, München, Germany.
- Stubbs, M. T., Laber, B., Bode, W., Huber, R., Jerala, R., Lenarcic, B. & Turk, V. (1990). *EMBO J.* **9**, 1939–1947.
- Tomlinson, G. E. & Kim, S. H. (1981). *J. Biol. Chem.* **256**, 12476–12477.
- de Vos, A. M., Hatada, M., van der Wel, H., Krabbendam, H., Peerdeman, A. F. & Kim, S. H. (1985). *Proc. Natl Acad. Sci. USA*, **82**, 1406–1409.
- van der Wel, H. (1972). *FEBS Lett.* **21**, 88–90.
- van der Wel, H., Hladik, A., Hladik, C. M., Hellikant, G. & Glaser, D. (1989). *Chem. Senses*, **14**, 75–79.
- van der Wel, H. & Loeve, K. (1972). *Eur. J. Biochem.* **31**, 221–225.
- Wlodawer, A. & Hodgson, K. O. (1975). *Proc. Natl Acad. Sci. USA*, **72**, 398–399.
- Wlodawer, A., Nachman, J., Gilliland, G. L., Gallagher, W. & Woodward, C. (1987). *J. Mol. Biol.* **198**, 469–480.
- Yamashita, H., Theerasilp, S., Aiuchi, T., Nakaya, K., Nakamura, Y. & Kurihara, Y. (1990). *J. Biol. Chem.* **265**, 15770–15775.